



## Manufacture of tablets with structurally-controlled drug release using rapid tooling injection moulding

Erin Walsh<sup>a,b</sup>, Natalie Maclean<sup>a,b</sup>, Alice Turner<sup>a,b</sup>, Moulham Alsuleman<sup>a,b</sup>, Elke Prasad<sup>a,b</sup>, Gavin Halbert<sup>a,b</sup>, Joop H. ter Horst<sup>a,b,c</sup>, Daniel Markl<sup>a,b,\*</sup>

<sup>a</sup> Strathclyde Institute of Pharmacy and Biomedical Sciences, University of Strathclyde, Glasgow, UK

<sup>b</sup> Centre for Continuous Manufacturing and Advanced Crystallisation (CMAC), University of Strathclyde, Glasgow, UK

<sup>c</sup> Laboratoire Sciences et Méthodes Séparatives, Université de Rouen Normandie, Mont Saint Aignan Cedex, France

### ARTICLE INFO

#### Keywords:

Injection moulding  
Rapid tooling  
Specific surface area  
Additive manufacture  
Dissolution

### ABSTRACT

With advancements in the pharmaceutical industry pushing more towards tailored medicines, novel approaches to tablet manufacture are in high demand. One of the main drivers towards micro-scale batch production is the ability to fine-tune drug release. This study demonstrates the use of rapid tooling injection moulding (RTIM) for tablet manufacture. Tablets were manufactured with varying structural features to alter the surface area whilst maintaining the same volume, resulting in differing specific surface area (SSA). The precision of this technique is evaluated based on eleven polymer formulations, with the tablets displaying <2% variability in mass. Further tablets were produced containing paracetamol in three different polymer-based formulations to investigate the impact of SSA on the drug release. Significant differences were observed between the formulations based on the polymers polyvinyl alcohol (PVA) and Klucel ELF. The polymer base of the formulation was found to be critical to the sensitivity of the drug release profile to SSA modification. The drug release profile within each formulation was modified by the addition of structural features to increase the SSA.

### 1. Introduction

The interest in manufacturing micro-scale batches of pharmaceutical products continues to heighten with the growth of the personalised medicine and clinical trials market. The development and manufacture of products for small patient populations using traditional large scale industrial production processes is currently not cost effective and hence hinders the progress in this area. Novel technologies to manufacture micro-scale batches in a sustainable manner are needed. One such technique is additive manufacturing (AM), commonly referred to as 3D printing. This technique is able to produce tablets with complex geometries allowing formulators to adjust the dose and modify the drug release profiles by varying the specific surface area of the dosage form (Goyanes et al., 2015; Karasulu and Ertan, 2002). Another manufacturing technology with potential to produce micro-scale batches is injection moulding (IM) coupled with hot melt extrusion (HME). IM is a widely applied manufacturing technique in the plastics industry and has been utilised in the pharmaceutical industry to produce solid oral dosage forms (Bartlett et al., 2017; Quinten et al., 2009; Zema

et al., 2012). The manufacturing benefits of using IM to make pharmaceutical drug products include reduced microbial contamination alongside greater freedom in defining the size and shape of the dosage form (Zema et al., 2012). In addition, IM allows the production of solid dispersions and solutions which can increase the rate of release of the drug and hence improve bioavailability (Quinten et al., 2009). This aspect is critically important for current and future medicines as approximately 70% of new drug candidates in the development pipeline show poor solubility (Loftsson and Brewster, 2010).

The IM process uses heat to encourage a thermoplastic material to adopt the desired geometry. Thermoplastics are a particularly large collection of materials with unique thermal, mechanical and electrical characteristics (Giboz et al., 2007; Hecke and Schomburg, 2004). The differing material properties of these thermoplastic materials therefore need to be understood to utilise them effectively in an IM-based process. Pressure-volume-temperature behaviour, polymer structure, morphology and crystallinity are all material properties that will have a major impact on the IM process (Annicchiarico and Alcock, 2014). A number of process parameters involved in IM impact the viscosity of the

\* Corresponding author.

E-mail address: [daniel.markl@strath.ac.uk](mailto:daniel.markl@strath.ac.uk) (D. Markl).

<https://doi.org/10.1016/j.ijpharm.2022.121956>

Received 29 January 2022; Received in revised form 20 June 2022; Accepted 21 June 2022

Available online 24 June 2022

0378-5173/© 2022 The Authors. Published by Elsevier B.V. This is an open access article under the CC BY license (<http://creativecommons.org/licenses/by/4.0/>).

thermoplastic material such as shear stress, shear rate, temperature and pressure.

Besides the solubility of the drug substance, the drug release of oral solid dosage forms made through IM are influenced by the formulation and the specific surface area (SSA) (Goyanes et al., 2015; Martinez et al., 2018; Quinten et al., 2009). The SSA can be modified by adjusting the surface area of the tablet while keeping the volume constant. Alterations to the SSA can be achieved by designing structural features into the surface of the tablet, which can be realised using micro-IM. Micro-IM is used when an object contains either a mass of a few milligrams,  $\mu\text{m}$ -scale features or objects where dimensional tolerances are in the  $\mu\text{m}$  range (Giboz et al., 2007; Packianather et al., 2015).

The IM process (standard and micro) requires an appropriate mould that defines the shape of the final product. Traditional metal mould-making is a time-consuming process which is both cost and skill exhaustive (Rani et al., 2018). In most cases this limits the optimisation of moulds, which is a crucial step in identifying a suitable product structure with micro-features that meet the performance specifications. Requirements for the fabrication of the mould and its material include the ability to create precise micro-structures and it must be sufficiently hard and ductile to survive the injection moulding process (Heckele and Schomburg, 2004). Developments in additive manufacturing have opened the door for rapid tooling in IM as an alternative to traditional metal moulds (Rani et al., 2018). Rapid tooling is defined as being the use of additive manufacturing techniques for the manufacture of moulds directly (direct tooling) or to create a pattern which is then used to manufacture a mould (indirect tooling) (Mendible et al., 2017; Qayyum et al., 2017; Rani et al., 2018). With additive manufacturing techniques now utilising photopolymers to print objects with high resolution, the potential for this technique to be used to manufacture moulds for micro-IM is apparent (Mohan et al., 2017; Surace et al., 2021). In order for these materials to be suitable for use in micro-IM, there must be sufficient resistance to both the temperature and pressure experienced during the injection process (Bartlett et al., 2017). Photopolymer-based additive manufacturing techniques were selected due to the material properties of the photoresins used, i.e. photoresins are expected to have high thermal resistance and superior surface quality making them a good choice for rapid tooling (Bartlett et al., 2017). Previous work by Walsh et al. (2021) demonstrated that stereolithography (SLA) can produce mould inserts suitable for use in conjunction with IM and suggests printing recommendations for this purpose. The integration of rapid tooling and injection moulding (Rapid Tooling Injection Moulding or RTIM) reduces the overall cost and the lead-time that comes with using traditional metal moulds (Formlabs, 2016; Mendible et al., 2017). The coupling of these technologies makes low production runs economically feasible and also allows for a more agile approach to research (Formlabs, 2016; Mendible et al., 2017).

The objectives of this work were to develop a process for producing solid oral dosage forms with structural features designed to control SSA using the RTIM technique and assess its suitability for adjusting the drug release behaviour. Three different geometries of dosage forms were produced using ten different pharmaceutical grade polymers which are typically used in HME, IM and additive manufacture. The relationship between drug release and SSA was assessed for three different paracetamol formulations, each containing a different polymer. The processability of these materials was assessed as was the accuracy and precision of the process in reference to the digital design of the tablets.

## 2. Materials and methods

### 2.1. Materials

#### 2.1.1. Stereolithography additive manufacture

The photoresin used in this work is Clear v4 from Formlabs (Massachusetts, USA) based on the findings from (Walsh et al., 2021). Isopropyl alcohol (Sigma Aldrich, USA) is used to wash the moulds post-

printing.

#### 2.1.2. Rapid tooling injection moulding

A number of raw materials were used in this work as detailed in Table 1. The materials used are pharmaceutical-grade with the exception of LDPE. LDPE is included as a reference material as it has been widely studied in the literature of IM and micro-IM. The acronym for each material will be used throughout this manuscript to refer to a particular material.

The majority of the formulations used in this work required preparation via HME to ensure molecular level mixing prior to feeding the material into the RTIM system. A series of formulations comprised solely of polymers or polymers with plasticising agents were produced and are detailed in Table 2. The API-containing formulations used in this work are detailed in Table 3.

### 2.2. Methods

#### 2.2.1. Stereolithography additive manufacture

Mould inserts were printed, as previously reported, using the Form 2 (Formlabs, Massachusetts) SLA printer (Walsh et al., 2021). The moulds are printed at a 45° angle from the build platform. On completion of printing, the moulds were washed in isopropyl alcohol in an agitated wash bath for a period of 10 min before being left to dry completely. The moulds were then removed from the build platform and placed in the FormCure (Formlabs) for 60 min at 60 °C. Supporting material was removed and any surface roughness on the rear of the mould surface was lightly sanded.

#### 2.2.2. Design of tablet geometries

Three different mould insert designs were produced for this study (see Fig. 1)) to modify the tablet geometry. Conical frustum shaped 'pins' (Fig. 2c) were added to the designs in increasing number ( $n = 2, 6$  or 10 for the three tablet geometries). In order to maintain the tablet mass across all three designs for a formulation, the volume of the three designs was kept constant. The diameter of the tablet was adjusted to account for the reduction in volume resulting from the introduction of the pins. The thickness of each tablet was kept constant for all three designs as were the dimensions of each pin.

The basic design of the tablet geometries comprised a cylindrical tablet with the conical frustum pins cut into the top surface (Fig. 2).

The surface area of the tablets was calculated using the following equation:

$$A_{\text{tab}} = 2\pi r_{\text{cyl}} h_{\text{cyl}} + 2\pi r_{\text{cyl}}^2 + n\pi \left[ r_{\text{pin1}}^2 - r_{\text{pin2}}^2 + (r_{\text{pin1}} + r_{\text{pin2}}) \sqrt{(r_{\text{pin1}} - r_{\text{pin2}})^2 + h_{\text{pin}}^2} \right], \quad (1)$$

**Table 1**

List of raw materials, their supplier details and their acronyms as used in this study.

Material	Supplier	Acronym
Affinisol HPMC HME 15LV	The Dow Chemical Company, USA	AFF
Eudragit E PO	Evonik, Germany	EPO
Klucel EF	Ashland, USA	KEF
Klucel ELF	Ashland, USA	KELF
Klucel LF	Ashland, USA	KLF
Low-density Polyethylene	Sigma Aldrich, USA	LDPE
Polyethylene	Sigma Aldrich, USA	PE
Polyethylene Glycol 4000	Sigma Aldrich, USA	PEG
Polyvinyl alcohol	Sigma Aldrich, USA	PVA
Soluplus®	BASF, Germany	SOL
Sorbitol Emprove Parteck SI 150	Merck, USA	SOR
Stearic Acid	Sigma Aldrich, USA	SA
Paracetamol	Mallinckrodt, UK	PCM

**Table 2**

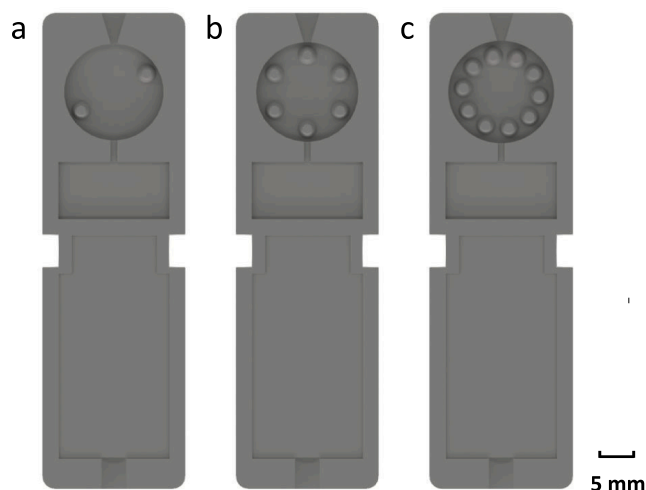
List of polymer-based formulations, their preparation method and their acronyms that will be used in this manuscript. Composition ratios are given in brackets by weight.

Primary Polymer	Plasticiser	Prep Method	Acronym
Affinisol	–	HME	AFF
Affinisol (85%)	Polyethylene Glycol (15%)	HME	AFF/PEG 85/15
Affinisol (85%)	Stearic acid (15%)	HME	AFF/SA 85/15
Affinisol (85%)	Polyethylene (15%)	HME	AFF/PE 85/15
Eudragit EPO (85%)	Polyethylene Glycol (15%)	HME	EPO/PEG 85/15
Klucel EF	–	HME	KEF
Klucel ELF	–	HME	KELF
Klucel LF	–	HME	KLF
Polyvinyl Alcohol	–	HME	PVA
Soluplus (85%)	Sorbitol (15%)	HME	SOL/SOR 85/15

**Table 3**

List of paracetamol formulations and their acronyms that will be used in this manuscript. Composition ratios are given in brackets by weight.

Formulation	Acronym
Affinisol (50%) + Paracetamol (50%)	AFF/PCM 50/50
Klucel ELF (90%) + Paracetamol (10%)	KELF/PCM 90/10
Polyvinyl Alcohol (90%) + Paracetamol (10%)	PVA/PCM 90/10

**Fig. 1.** The three mould designs used in this study. a) 2 Pin b) 6 Pin c) 10 Pin.

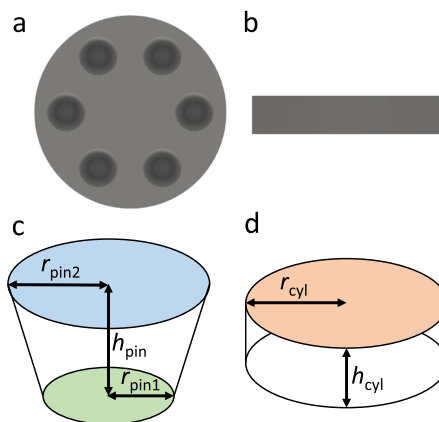
where  $A_{\text{tab}}$  is the tablet surface area,  $r_{\text{cyl}}$  is the radius of the cylinder,  $h_{\text{cyl}}$  is the height of this cylinder,  $n$  is the number of pins,  $r_{\text{pin1}}$  is the top radius of the pin,  $r_{\text{pin2}}$  is the bottom radius of the pin and  $h_{\text{pin}}$  is the depth of the pin.

The volume of the tablets was calculated using the following equation:

$$V_{\text{tab}} = 2\pi r_{\text{cyl}}^2 h_{\text{cyl}} - \left( \frac{1}{3} \pi n h_{\text{pin}} (r_{\text{pin1}}^2 + r_{\text{pin2}}^2 + r_{\text{pin1}} r_{\text{pin2}}) \right), \quad (2)$$

where  $V_{\text{tab}}$  is the tablet volume,  $r_{\text{cyl}}$  is the radius of the cylinder,  $h_{\text{cyl}}$  is the thickness of the cylinder,  $n$  is the number of pins,  $h_{\text{pin}}$  is the depth of the pin,  $r_{\text{pin1}}$  is the top radius of the pin and  $r_{\text{pin2}}$  is the bottom radius of the pin.

The specific surface area was calculated as the ratio between the surface area to the volume:

**Fig. 2.** Schematic of tablet design features. a) A top and b) side view of a tablet produced from the 6 Pin design; c) design of an individual pin; d) design of the basic cylindrical tablet structure.

$$SSA_{\text{tab}} = \frac{A_{\text{tab}}}{V_{\text{tab}}} \quad (3)$$

Full details of the tablet dimensions produced from these designs can be found in Table 4.

### 2.2.3. Rapid tooling injection moulding

The RTIM process couples SLA with IM. Mould inserts, produced via SLA, are housed within a metal mould casing (Fig. 3). Also visible are a number of design features on the printed mould insert to make it suitable for use in the RTIM process. The tablet cavity is the section of the mould insert which will produce the tablet. The air cavity provides an overflow space for any excess injection material and offers a space for the air to compress upon moulding. The removal points can be found on each side of the mould, these aid in removing the mould inserts from the metal moulds. The separation point at the bottom of the mould inserts is used to separate the two halves of the mould insert.

The two halves of the metal mould were pieced together and placed into the HAAKE MiniJet Pro Piston Injection Moulding System (Thermo Fisher Scientific, USA) which is an upright air-pressurised injection moulder. The injection material is placed into the melt cylinder, the piston is attached and this is then placed into the injection moulder. A number of processing parameters must be set:

- Cylinder temperature to which the injection material will be heated to.
- Mould temperature to which the mould will be heated to.
- Injection pressure which will be applied to the piston to move the injection material into the mould.
- Injection time is the length of time for which the injection pressure will be applied.
- Hold pressure which will be applied after the injection material has filled the mould.

**Table 4**

Summary table of tablet dimensions.

Design Feature	2 Pin Design	6 Pin Design	10 Pin Design
Diameter (mm)	15.23	15.69	16.12
Thickness (mm)	3	3	3
Volume (mm <sup>3</sup> )	530.03	529.82	529.80
Surface Area (mm <sup>2</sup> )	527.48	592.76	658.08
Number of Pins	2	6	10
Pin Depth (mm)	2	2	2
Pin Radius 1 (mm)	1.5	1.5	1.5
Pin Radius 2 (mm)	0.75	0.75	0.75
Specific Surface Area (mm <sup>-1</sup> )	1.00	1.12	1.24

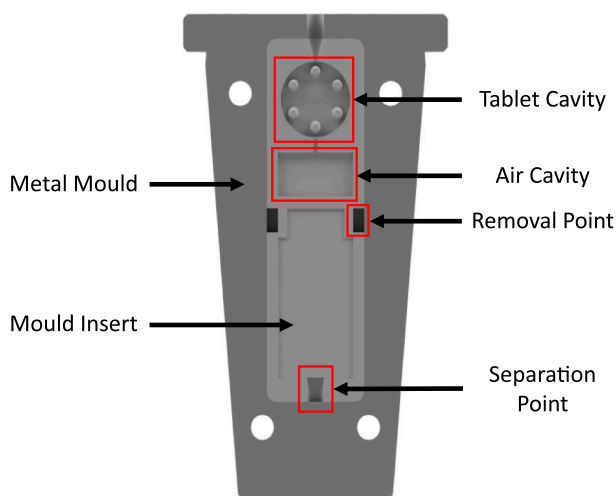


Fig. 3. The mould insert for the 6 Pin Design inserted into the metal mould. This depiction represents one half of the full mould.

- Hold time is the length of time for which the hold pressure will be applied.

These processing parameters vary for different injection materials (see Table 5). For all formulations the injection time, hold pressure and hold time were kept constant at 10 s, 50 bar and 10 s, respectively.

A number of formulations (see formulations marked with \* in Table 5) required the application of a silicone based lubricant onto the surface of the mould inserts to aid removal of the injected material. Upon completion of injection, the metal mould is removed from the injection moulder, the metal mould opened and the mould insert removed. When sufficiently cooled, the mould insert is opened and the tablet removed from the mould cavity.

#### 2.2.4. Gravimetric analysis

All tablets were weighed on a four decimal point balance (Entris II, Sartorius). The masses reported reflect the average of each batch produced. The mean and standard deviations reported are  $n = 60$  for LDPE and  $n = 18$  for all other formulations.

#### 2.2.5. Dimensional analysis

The diameter and thickness of each tablet was measured using a digital calliper (Scienceware Digi-Max, Sigma Aldrich). A total of three diameter and three thickness measurements were taken for each tablet,

Table 5

RTIM process parameters used for each of the formulations. Formulations marked with \* required the addition of an aerosol silicone-based lubricant to aid removal from the mould. The API-containing formulations are given below the double horizontal line.

Formulation	Cylinder Temp	Mould Temp	Injection Pressure
AFF*	N/A	N/A	N/A
AFF/PEG 85/15*	200 °C	100 °C	150 bar
AFF/SA 85/15*	180 °C	100 °C	150 bar
AFF/PE 85/15*	180 °C	100 °C	150 bar
EPO/PEG 85/15*	N/A	N/A	N/A
KEF	140 °C	70 °C	150 bar
KELF	140 °C	70 °C	150 bar
KLF	140 °C	70 °C	150 bar
PVA*	200 °C	70 °C	200 bar
SOL/SOR 85/15*	N/A	N/A	N/A
AFF/PCM 50/50*	130 °C	70 °C	150 bar
KELF/PCM 90/10*	120 °C	70 °C	150 bar
PVA/PCM 90/10*	180 °C	100 °C	200 bar

the measurements shown are an average of these replicates. The mean and standard deviations reported were  $n = 60$  tablets for LDPE and  $n = 18$  for all other formulations.

#### 2.2.6. Optical coherence tomography

A spectral-domain optical coherence tomography (OCT) system (GAN600 Series, Thorlabs, New Jersey, USA) equipped with a LK3-BB (focal length: 36 mm) was used to measure the actual pin dimensions. OCT produces cross-sectional images of a sample which can be used for depth measurements. The lateral resolution is  $\approx 4 \mu\text{m}$ , the axial resolution in air is  $\approx 3 \mu\text{m}$  and the image size is  $1024 \times 1024$  pixels with a x-axis pixel size of  $5.86 \mu\text{m}$  and a y-axis pixel size of  $1.95 \mu\text{m}$ . The OCT probe was focused over the pins on the tablet surface and a 2D cross-section image was acquired. The focus is adjusted to ensure a strong signal. The diameters (see Fig. 2c) at both the top and bottom surfaces and the depth of the pins were measured. The mean and standard deviations are reported for 18 samples for all formulations.

#### 2.2.7. Dissolution

Dissolution testing was performed using an ADT8i Dissolution bath (USP II) paddle on a closed loop setting with a T70+ UV/Visible spectrophotometer (Automated Lab Systems, UK). Each vessel contained 1000 mL of 50 mM  $\text{KH}_2\text{PO}_4$  adjusted to pH 5.8 with NaOH. Dissolution testing was performed at 37 °C with a paddle speed of 50 rpm. Samples were automatically drawn at a rate of 20 mL/min through the sampling pump with a flush volume of 20 mL and with cannula filters of  $20 \mu\text{m}$  (ALS, UHMW PE, Part No 50831). Samples were measured at timepoints of 5 min, 10 min, 15 min, 30 min, 1 h, 2 h, 4 h, 6 h and 8 h. UV detection of PCM was performed at a wavelength of 243 nm through a 1 mm flow cell cuvette. For each formulation, 6 tablets were tested. Standards of 0.2 mg/mL PCM in phosphate buffer were prepared in duplicate.

All tablets were weighed and their weights recorded. A standard verification of both PCM standards produced was performed prior to the dissolution assay, with the absorbance values for both standards recorded.

### 3. Results

#### 3.1. Gravimetric analysis

The mass across the three designs was designed to be constant for a given formulation as the volume was constant across the three tablet geometries. Variations of the calculated volume across the three designs were  $< 2.5\%$  across all formulations (Table S1-6 in the supplementary information). No data is shown for the AFF, EPO/PEG 85/15 and SOL/SOR 85/15 formulations as they were unprocessable via this RTIM process (more details are provided in the Discussion section). The average mass varied between formulations due to different true densities of the materials used. The variation in mass observed across all formulations and all designs was well within the pharmacopoeia standards ( $\pm 5\%$  of the tablet core weight) for tablet mass variation (Fig. 4a) The International Pharmacopoeia, 2019). Fig. 4b demonstrates the tablet to tablet variability within the LDPE tablets. A total of 60 tablets are displayed, showing that even within this larger batch size, the mass variation is low ( $\pm 0.58\%$ ) and the RTIM process produces consistent and uniform tablets.

Generally, a higher degree of variation was observed for the Affinisol-based formulations (Fig. 4c). This was attributed to the difficulty in processing these tablets. These formulations had a tendency to stick to the mould surface if not removed while warm leading to a reduced uniformity of mass compared to the other formulations tested. While the AFF/PEG formulation had the highest standard deviation across all formulations ( $\pm 1.87\%$ ), the masses still fell within the pharmacopoeia limits (Fig. 4b).

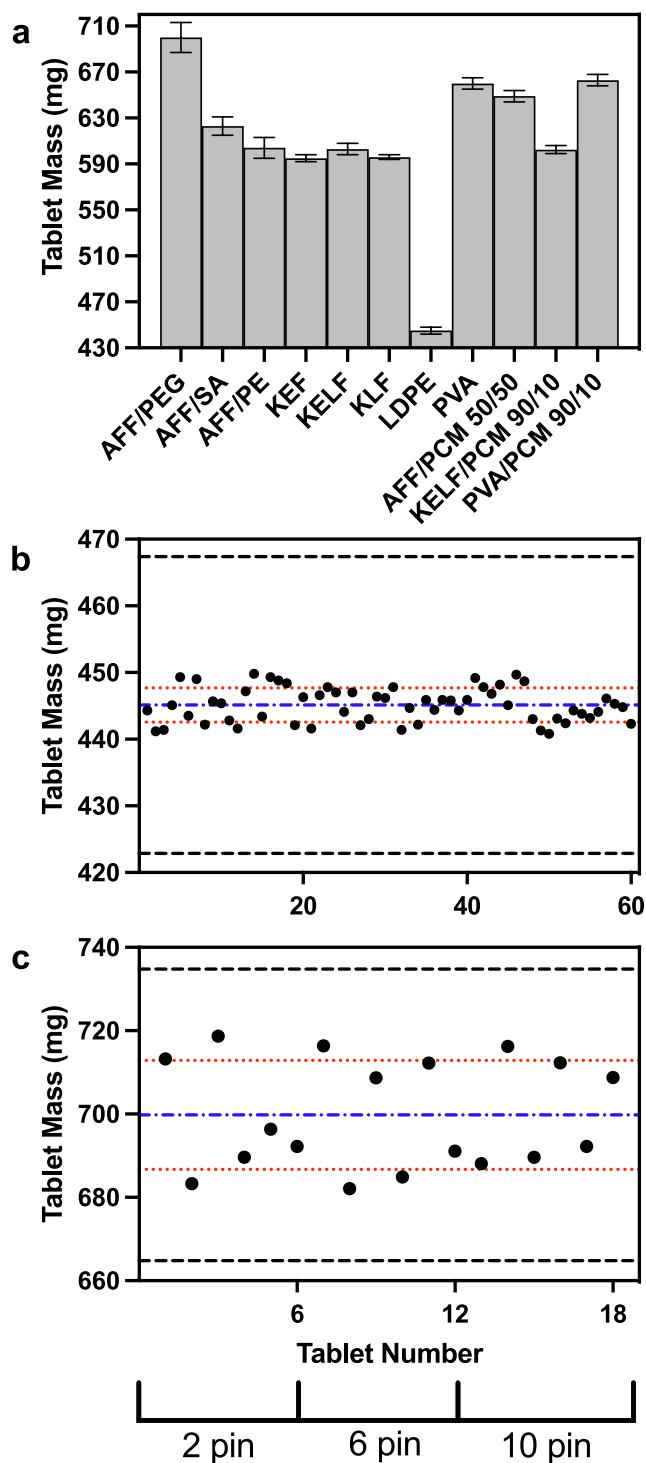


Fig. 4. Tablet mass of RTIM tablets. a) The average mass of all tablets for each formulation. Error bars represent the standard deviation ( $n = 60$  for LDPE,  $n = 18$  for all other formulations). b) The mass of 60 LDPE tablets. c) the mass of 18 AFF/PEG tablets. The blue dotted lines represent the average tablet weight of this batch with the upper and lower red dotted lines being the average plus or minus the standard deviation respectively. The black dotted lines represents the upper and lower pharmacopoeia limit (in this case taken as tablet weight  $\pm 5\%$ ).

### 3.2. Dimensional analysis

All formulations demonstrated high accuracy and precision to the digital designed thickness value of 3 mm, i.e.  $<99.84\%$  of designed value with a standard deviation of  $\pm 0.88\%$  across all formulations and

geometries. The Affinisol-based formulations produced values slightly higher than the design value (100.70% of design) and the measurements had a slightly higher standard deviation ( $\pm 0.81\%$ ) than for non-AFF based formulations ( $\pm 0.30\%$ ) which is attributed to the difficulty associated with processing these formulations as previously discussed. As above, no data is shown for the AFF, EPO/PEG 85/15 and SOL/SOR 85/15 formulations.

All formulations demonstrated good accuracy and precision to the digital designed diameter values across all three tablet geometries (ranging from  $98.68 \pm 0.42\%$  to  $99.71 \pm 0.23\%$  of the intended values).

The depth, top diameter and bottom diameter of the pins in all three geometries were measured using OCT. Both the depth of the pins and the bottom diameter (as seen in Fig. 5a and c respectively) were below the

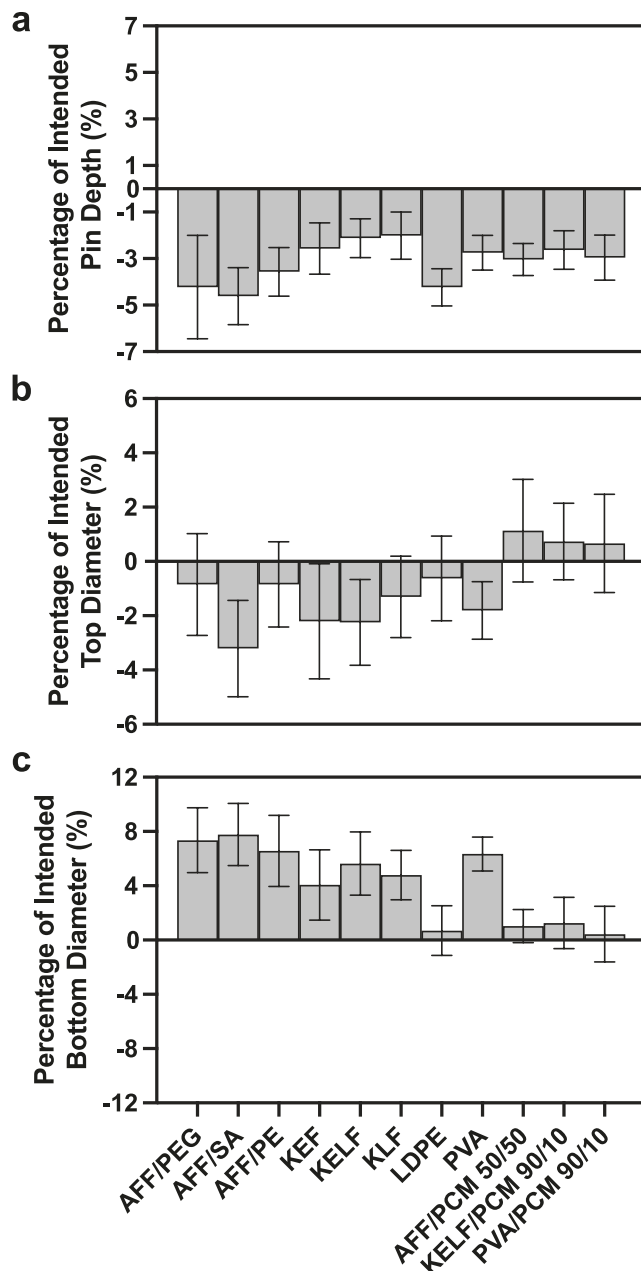


Fig. 5. Tablet pin characteristics measured by OCT. a) The depth of the pins on the tablet surface ( $h_{pin}$  from Fig. 2c) b) The top surface diameter of the pins on the tablet surface ( $2 \times r_{pin1}$  from Fig. 2c) c) The bottom surface diameter of the pins on the tablet surface ( $2 \times r_{pin2}$  from Fig. 2c) a-c: for each bar  $n = 6$  measurements with the error bars representing the standard deviation.

expected values across all formulations. The top diameter of the pins (as seen in Fig. 5b) was generally above the expected value of 3 mm across all formulations. While the measured values deviated slightly from the designed values, the low values of the standard deviations across all measurements suggest that the variability within the batches was small.

Fig. 6 displays the three tablet geometries for PVA and AFF/SA formulations. It is worth noting that for the AFF based formulations, the RTIM process is not considered optimised and the colouration on the tablets produced is indicative of thermal degradation of the AFF polymer. Reduction of the processing temperatures would reduce this polymeric degradation and result in dosage forms having a lighter colour.

From the dimensional analysis, the surface area, volume and specific surface area (Fig. 7) were calculated using Eqs. (1)–(3). Full details of the equations used to calculate these parameters and the propagation of errors can be found in section S2 of the supplementary information.

### 3.3. Dissolution

Dissolution studies were conducted for each tablet geometry on the three PCM formulations (Fig. 8). From this study, no significant differences in the drug release profiles of AFF/PCM 50/50 could be detected from the three tablet geometries trialled. On the contrary, significant differences in the rate of drug release were observed between the different tablet geometries for KELF/PCM 90/10 (Fig. 8b) and PVA/PCM 90/10 (Fig. 8c) formulations.

Due to the asymmetric nature of the dosage forms produced in this work, there are two distinct faces. The release profile can be influenced by the orientation of the tablet in the dissolution vessel. Only dissolution data of tablets with the face up (pins on top) were used in the results shown here. The first face is that which has the pins indented into the

surface, and the second face is the flat cylindrical base. This asymmetry of the tablets presented some challenges during the dissolution studies. All of the tablets were positioned with the pin-face upwards when the dissolution studies were conducted. The system which was used for this work operates to drop the tablets into the dissolution vessels simultaneously. When the tablets fall, some come to rest in the base of the vessels with the pin-face upwards, and others with the pin-face downwards (see Fig. 9a). The tablets which were pin-face downwards demonstrated slower drug release (see Fig. 9b), which is attributed to the reduced access of the dissolution media to the surface micro-features and differing hydrodynamics on the two faces of the tablet.

For future studies, the tablets could manually be placed into the dissolution vessels to avoid these inconsistencies. Putting micro-features on both faces of the tablet surface would likely reduce the errors associated with the asymmetry. However, the blocked face would still have limited liquid access and therefore the full impact of the increase in SSA would not be clear from such a set up. It is however worth stating that this issue is not an issue that would be encountered in vivo.

## 4. Discussion

### 4.1. Formulation processability in RTIM

Three of the formulations trialled were deemed to be unprocessable: AFF, EPO/PEG 85/15 and SOL/SOR 85/15. For the AFF formulation, the main challenge was associated with the temperatures and pressures required to process the material. The temperatures and pressures required to achieve a workable viscosity of the formulation were too high for the mould materials to withstand, causing fracture of the plastic mould inserts and ultimately resulting in an unsuccessful RTIM process. EPO/PEG 85/15 and SOL/SOR 85/15, adhered strongly to the surface of

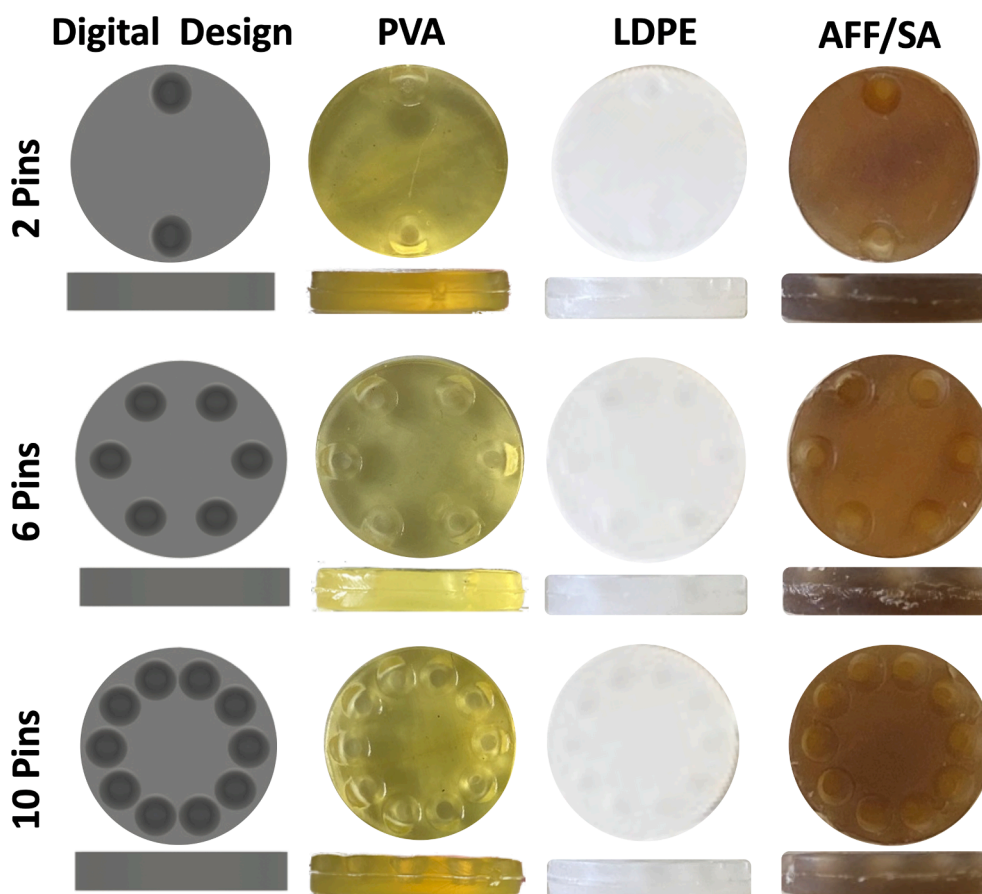


Fig. 6. Physical tablets produced for three of the formulations trialled.

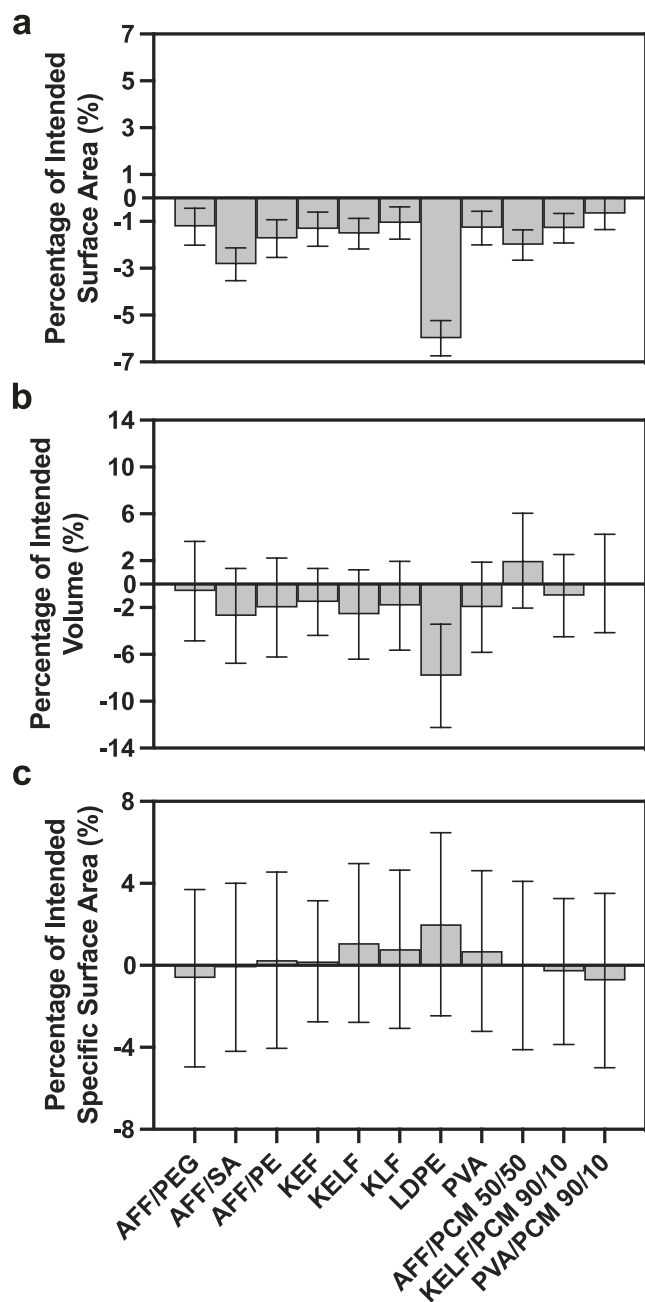


Fig. 7. Analysis of the actual surface area, volume and specific surface area compared to the digital design. a) The average surface area for each formulation as calculated by Eq. 1. b) The average volume for each formulation as calculated by Eq. 2. c) The average specific surface area for each formulation as calculated by Eq. 3. a-c: for each bar,  $n = 60$  tablets for LDPE and  $n = 18$  for all other formulations with the error bars representing the propagated standard deviation.

the printed mould. While this is an issue that was encountered with a number of other formulations (those marked with \* in Table 5), the addition of the silicon-based lubricant was not able to overcome the issues. For the EPO/PEG 85/15 and SOL/SOR 85/15 formulations a number of processing parameters were trialed including varying the temperatures for both the cylinder and the mould, reducing the injection pressure and the injection time. No successful processing conditions could be found for these materials in this specific RTIM process. The extent of the adhesion to the printed mould surface was such that the two mould halves were fused together. As such, removal of the tablets from these moulds was not possible and the formulations were deemed

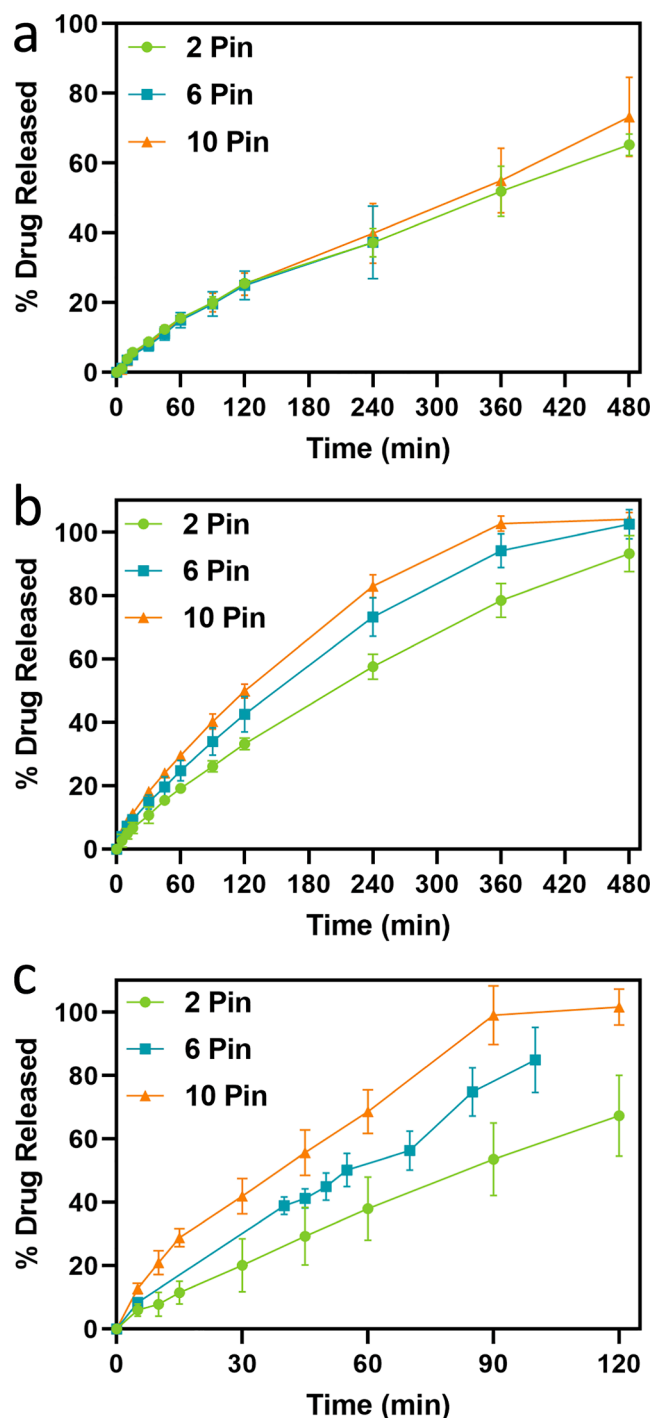


Fig. 8. Drug release profiles for a) AFF/PCM 50/50, b) KELF/PCM 90/10 formulation and c) PVA/PCM 90/10 formulation. All: Symbols represent the mean of  $n = 6$  tablets (with the exception of PVA/PCM 90/10, for which  $n = 4$ ) with the error bars showing 95% confidence intervals. In b), data collection of AFF/PCM 50/50 formulations was terminated after the 240 min time point for the 6 Pin geometry due to errors with the dissolution apparatus. In c), the sample time points for the 6 Pin geometry differ to those of the 2 Pin and 10 Pin geometries due to running errors with the dissolution apparatus.

unprocessable. Further studies could investigate whether inclusion of a gap in the mould design would prevent the mould from fusing and facilitate the separation of the mould and removal of the tablet for formulations which are prone to high levels of adhesion.

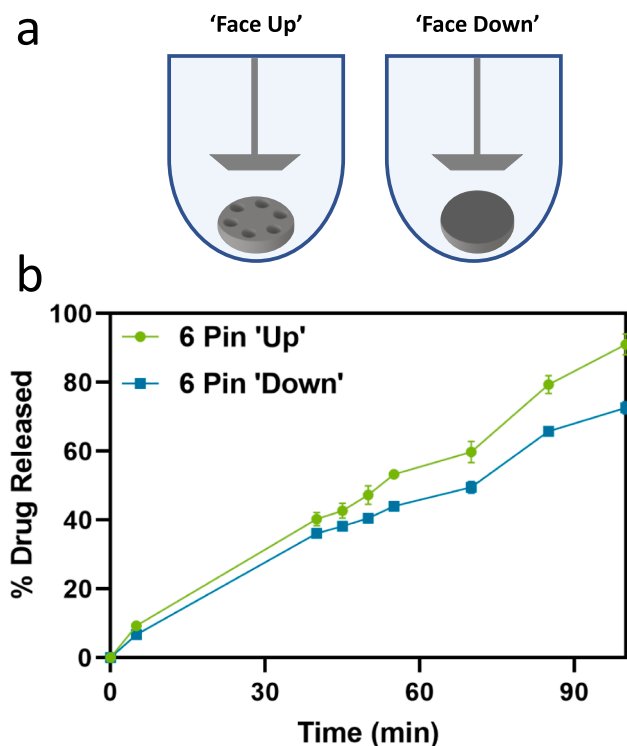


Fig. 9. Impact of anisotropic tablet structure on drug release profiles of the PVA/PCM 90/10 formulation. a) A depiction of the 'Face Up' and 'Face Down' orientation that tablets may adopt in the dissolution vessels b) 6 Pin PVA/PCM 90/10 tablets split by 'Face up' and 'Face down'. Sample size for 'Face up' is 4 tablets and for 'Face down' is 2 tablets. Error bars represent the 95% confidence intervals.

#### 4.2. Physical Parameters of the tablets

Theoretically, all formulations should produce physical parameters which match the digital design. The digitally designed volume was constant across the three geometries, while the surface area and specific surface area increased with the increased number of pins.

There are a number of factors which create uncertainty in these calculated values. Primarily, there is an inherent uncertainty that arises from the printing of the plastic mould inserts which was extensively studied in (Walsh et al., 2021). Additionally, there are measurement errors associated with the different techniques used to measure the dimensions of the tablets. The uncertainty arising from the measurements alone attributes 22.79% of the uncertainty on volume, 24.11% for surface area and 22.82% for specific surface area. Finally, there are errors associated with the different formulations used. This is most apparent when looking at the mass variability of the formulations, where some have significantly higher standard deviations than others. The only variable changed in that case is the formulation so it can be assumed that the difference in standard deviation is attributed solely to the formulation differences. These formulation differences are likely driven by density differences between the formulations, caused by different polymer structures, rheology and packing, as well as the interactions between the polymers and plasticisers. It may be possible that these effects could be mitigated by incorporating a correction factor to adjust the mould design for a given formulation.

Fig. 7a and b depicts the calculated values for surface area, volume and specific surface area for all formulations. The specific surface area demonstrated high accuracy and precision across all formulations trialled. With the exception of LDPE, both the surface area and volume data demonstrate a high degree of both accuracy and precision to the digital design. The LDPE formulation was found to have a lower surface

area and volume than the digital design. The accuracy of the LDPE formulation was therefore lower than the others tested however the precision of the measurements remained high. As polyethylene (and therefore LDPE) is a semi-crystalline thermoplastic, this can be attributed to shrinkage on cooling which is characteristic of crystalline polymers (De Santis et al., 2010). While the shrinkage resulting in a reduced diameter was clear, there was some evidence of the thickness value also being lower than anticipated and lower than all other formulations tested. This shrinkage is expected to be highest on the longest axis which for these designs would be the diameter. The specific surface area demonstrated high accuracy and precision across all formulations trialled. Even in the case of LDPE, where reduced accuracy was observed for surface area and volume, the deficit to both was such that the specific surface area fell much closer to the digitally designed value.

The relationship between the number of pins featured in the design and the resultant specific surface area is highly linear producing an  $R^2$  of 0.99 based on the data collected for all formulations trialled in this study (Fig. 10). This indicates that further modification of the specific surface area could be achieved via this pin-based approach with a high degree of accuracy.

#### 4.3. Drug release analysis

The AFF/PCM 50/50 formulation generally had a slow drug release, failing to reach 100% release after the 8 h time period the dissolution test was conducted for. Based on the data collected, the AFF/PCM 50/50 results do not show a clear difference in drug release rate for tablets with 2, 6 or 10 pins. A similar study by Prasad et al. (2019) assessed the dissolution performance of 3D printed AFF tablets containing 10% and 50% wt. PCM. In this study, different tablet geometries (cylindrical, rectangular grids with and without slotted shapes) with different SSAs were manufactured. It was demonstrated that drug release was fastest with increasing SSA for these designs (Prasad et al., 2019), whereas the AFF/PCM tablets tested in this study do not follow the same trend. This may be attributed to the large dose of PCM (~320 mg for AFF/PCM, compared to ~60 mg for PCM/KELF and PCM/PVA formulations, and 17 and 80 mg in the AFF-based formulations tested by Prasad et al. (2019)). It should also be noted that the release behaviour can be influenced by the manufacturing method and hence differences in the drug release profiles between the 3D printed tablets and the RTIM tablets may not exclusively be caused by the different drug loadings.

Significant differences were observed across the drug release profiles of both KELF/PCM 90/10 and PVA/PCM 90/10 formulations with different numbers of pins. This finding is in agreement with other studies, in which increasing SSA was found to increase the rate of drug release (Goyanes et al., 2015; Reynolds et al., 2002). The time to reach 50% drug release for each formulation is shown in Fig. 11. For

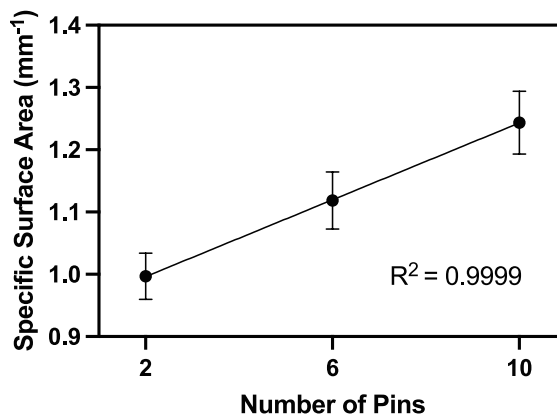


Fig. 10. The average specific surface area for all formulations vs. the number of pins in the tablet geometry. Error bars represent the standard deviation.

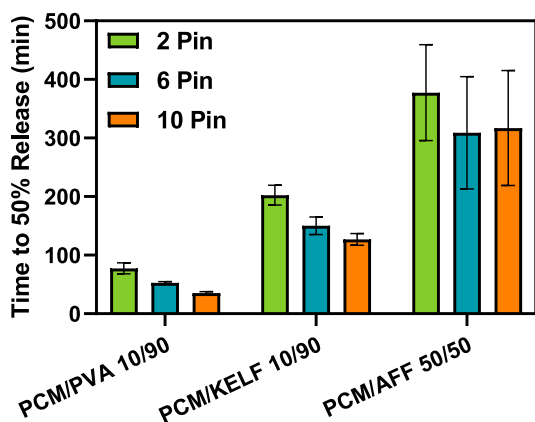


Fig. 11. The time taken for formulations to reach 50% drug release for each formulation split by tablet geometry.

formulations containing PVA and KELF, increasing the SSA resulted in a decrease in the time to release 50% of the drug. As discussed above, this trend is not displayed for the AFF-based formulation. This suggests that the polymer used in the formulation has a significant impact on both the sensitivity to changes in SSA and the absolute time for drug release. This could be attributed to the higher dose of PCM in the AFF formulation compared to KELF or PVA-based tablets. The mechanism of drug release influences the sensitivity to changes in SSA (e.g. diffusion, erosion, and swelling), however further studies would be required to investigate the release mechanisms as these can be influenced by the API, formulation, tablet size and geometry, and the manufacturing process.

#### 4.4. Capabilities and limitations of RTIM for solid oral dosage form fabrication

RTIM produces tablets with very low interparticle (uncontrolled) porosity within the dosage form that enables a tight control of the available surface area and hence release behaviour. Even minor changes in the surface area can thus influence the release behaviour as shown in this study.

Additionally, RTIM presents the potential for an increased formulation space, compared to other techniques that allow the customisation of the structure such as FDM. Typically, the drug loading that can be achieved for FDM printing is low due to the necessity for the print filament to possess the correct properties for successful printing (Zhang et al., 2018; Zhang et al., 2017; Korte and Quodbach, 2018; Aho et al., 2019). There have however been cases where a higher drug loading has been achieved (Prasad et al., 2019). Additionally, in most cases these filament properties also limit which polymers can be used in conjunction with FDM, further reducing the formulation space available for FDM (Zhang et al., 2018). Further work on material development will be required to expand the formulation space of FDM (Gioumouxouzis et al., 2019). For example, a recent paper by Zheng et al. (2021) demonstrated a novel 3D printing process that aims to mitigate some of the challenges of traditional FDM approaches and allows for the manufacture of tablets from excipient and API powders, without the need for filaments. RTIM on the other hand is not dependent on the filament properties and thus higher drug loadings and a wider range of polymer carriers can be used without further research and development. This will greatly expand the formulation space and allow a greater variety of drugs, drug loadings and polymers to be utilised for more complex dosage form geometries.

It must be mentioned that the RTIM process is not without its limitations. The major limitation of this technique is the current throughput. Both the RTIM and FDM processes require material preparation via hot melt extrusion, however RTIM also requires the printing of the mould inserts which adds significant time. The actual production of the tablets however is typically faster for RTIM, with a single tablet able to be

produced every 1–2 min while for FDM this is in the 4–5 min range (Korte and Quodbach, 2018; Zhang et al., 2017). Both of these times quoted would be for a formulation considered to be favourable, an unfavourable formulation would extend these production times further. The throughput of RTIM could be improved by utilising it as a development tool for a more traditional  $\mu$ IM process using a tooled steel mould. This would allow for a far more efficient process and enable the direct coupling with HME. While the structural flexibility for RTIM is considered high due to the ability to create accuracy and precise surface micro-features, it must also be noted that internal features would be far more difficult to produce. Therefore, there are structural and geometric limitations with the RTIM technique. Despite not having the constraints of the filament properties that FDM has, RTIM has additional limitations such as the material rheology and the tendency for some materials to stick to the mould inserts. Even with these drawbacks, the RTIM process displays clear potential to produce dosage forms with highly accurate and precise physical structures.

## 5. Conclusion

The RTIM method produced tablets from a variety of thermoplastic pharmaceutical grade polymers. These tablets were close to the digital designs in terms of their dimensions, surface area, volume and specific surface area. The mass variability of all tablets produced was low and well within the limits of the pharmacopoeia. The specific surface areas of the tablets produced were accurate to the digital designs suggesting that this RTIM process can be used to produce tablets of designed geometries for the purpose of fine-tuning drug release profiles. RTIM has proven to be an accurate and precise method for the production of tablets with a desired specific surface area.

The RTIM method was capable of producing drug-loaded tablets from pharmaceutical polymer-based formulations. It is well known that for many formulations, drug release kinetics are dependent on the specific surface area of the tablets (Goyanes et al., 2015; Martinez et al., 2018; Prasad et al., 2019; Pires et al., 2020). As such, to refine the drug release behaviour, the control of the specific surface area must be accurate. This has been achieved through addition and modification of pins into the tablet geometry and subsequent altering of the overall tablet diameter. The decision as to whether the RTIM process is the most appropriate is application dependent. Consideration of the accuracy, precision, material requirements and throughput amongst other factors should be carefully examined when deciding the most appropriate manufacture technique for the desired application. These factors will directly influence the throughput, cost and overall quality and trueness to the digital design. Evidence suggests that RTIM can be used successfully for low production runs of <500 parts, and for larger batches it can be used as a development tool to obtain the desired tablet design prior to producing a traditional tooled steel mould for scaled up production (Rahmati and Dickens, 2007).

## Declaration of Competing Interest

The authors declare the following financial interests/personal relationships which may be considered as potential competing interests: Erin Walsh reports financial support was provided by Engineering and Physical Sciences Research Council. Daniel Markl reports a relationship with The Royal Society that includes: funding grants..

## Acknowledgements

For the purpose of open access, the author has applied a Creative Commons Attribution (CC BY) licence to any Author Accepted Manuscript version arising from this submission. The authors would like to thank EPSRC and the Future Continuous Manufacturing and Advanced Crystallisation Research Hub (Grant Ref EP/P006965/1), EPSRC DTP (Grant Ref EP/N509760/1), EPSRC Strategic Equipment (Grant Ref EP/

S02168X/1), Royal Society (Grant Ref RSG/R2/180276) and the University of Strathclyde for funding this research. The authors would like to acknowledge that this work was carried out in the CMAC National Facility supported by UKRPIF (UK Research Partnership Fund) award from the Higher Education Funding Council for England (HEFCE) (Grant Ref HH13054). The data that was used to prepare the figures in this manuscript can be downloaded from the University of Strathclyde KnowledgeBase at <https://doi.org/10.15129/e1a516b3-41ad-4b38-81e1-6ebec17b8e7d>.

## Appendix A. Supplementary material

Supplementary data associated with this article can be found, in the online version, at <https://doi.org/10.1016/j.ijpharm.2022.121956>.

## References

- Goyanes, A., Martínez-Pacheco, R., Robles, P., Buanz, A., Basit, A.W., Gaisford, S., 2015. Effect of geometry on drug release from 3D printed tablets. *Int. J. Pharm.* 494, 657–663. <https://doi.org/10.1016/j.ijpharm.2015.04.069>.
- Karasulu, H.Y., Ertan, G., 2002. Different geometric shaped hydrogel theophylline tablets: Statistical approach for estimating drug release. *Farmaco* 57, 939–945. [https://doi.org/10.1016/S0014-827X\(02\)01297-1](https://doi.org/10.1016/S0014-827X(02)01297-1).
- Bartlett, L., Grunden, E., Mulyana, R., Castro, J., 2017. A Preliminary Study on The Performance of Additive Manufacturing Tooling for Injection Moulding. In: SPE ANTEC, 2017, pp. 100–104.
- Quinten, T., Beer, T.D., Vervae, C., Remon, J.P., 2009. Evaluation of injection moulding as a pharmaceutical technology to produce matrix tablets. *Eur. J. Pharm. Biopharm.* 71, 145–154. <https://doi.org/10.1016/j.ejpb.2008.02.025>.
- Zema, L., Loreti, G., Melocchi, A., Maroni, A., Gazzaniga, A., 2012. Injection Molding and its application to drug delivery. *J. Controlled Release* 159, 324–331. <https://doi.org/10.1016/j.jconrel.2012.01.001>.
- Loftsson, T., Brewster, M.E., 2010. Pharmaceutical applications of cyclodextrins: basic science and product development. *J. Pharm. Pharmacol.* 62, 1607–1621. <https://doi.org/10.1111/j.2042-7158.2010.01030.x>.
- Giboz, J., Copponex, T., Mélé, P., 2007. Microinjection molding of thermoplastic polymers: A review. *J. Micromech. Microeng.* 17, 96–109. <https://doi.org/10.1088/0960-1317/17/6/R02>.
- Heckele, M., Schomburg, W.K., 2004. Review on micro molding of thermoplastic polymers. *J. Micromech. Microeng.* 14. <https://doi.org/10.1088/0960-1317/14/3/R01>.
- Annicchiarico, D., Alcock, J.R., 2014. Review of factors that affect shrinkage of molded part in injection molding. *Mater. Manuf. Processes* 29, 662–682. <https://doi.org/10.1080/10426914.2014.880467>.
- Martinez, P.R., Goyanes, A., Basit, A.W., Gaisford, S., 2018. Influence of Geometry on the Drug Release Profiles of Stereolithographic (SLA) 3D-Printed Tablets. *AAPS PharmSciTech* 19. <https://doi.org/10.1208/s12249-018-1075-3>.
- Quinten, T., Beer, T.D., Remon, J.P., Vervae, C., 2009. Overview of Injection Molding As a Manufacturing Technique for Pharmaceutical Applications. *Innovation* 1–42.
- Packianather, M., Griffiths, C., Kadir, W., 2015. Micro injection moulding process parameter tuning. *Procedia CIRP*. <https://doi.org/10.1016/j.procir.2015.06.093>.
- Rani, A., Majdi, A., Altaf, K., Ahmad, F., Ahmad, J., 2018. Enhanced Polymer Rapid Tooling for Metal Injection Moulding Process. In: 3rd International Conference on Progress in Additive Manufacturing, pp. 656–661. <https://doi.org/10.25341/D4J014>.
- Mendible, G.A., Rulander, J.A., Johnston, S.P., Mendible, G.A., Rulander, J.A., Johnston, S.P., 2017. Comparative study of rapid and conventional tooling for plastics injection molding. *Rapid Prototyping J.* 23, 344–352. <https://doi.org/10.1108/RPJ-01-2016-0013>.
- Qayyum, J.A., Altaf, K., Abdul Rani, A.M., Ahmad, F., Jahanzaib, M., 2017. Performance of 3D printed polymer mold for metal injection molding process. *ARPN J. Eng. Appl. Sci.* 12, 6430–6434. <https://doi.org/10.3390/met8060433>.
- Mohan, M., Ansari, M.N., Shanks, R.A., 2017. Review on the Effects of Process Parameters on Strength, Shrinkage, and Warpage of Injection Molding Plastic Component. *Polym. Plast. Technol. Eng.* 56. <https://doi.org/10.1080/03602559.2015.1132466>.
- Surace, R., Basile, V., Bellantone, V., Modica, F., Fassi, I., 2021. Micro injection molding of thin cavities using stereolithography for mold fabrication. *Polymers* 13. <https://doi.org/10.3390/polym13111848>. URL: <https://www.mdpi.com/2073-4360/13/11/1848>.
- Walsh, E., ter Horst, J.H., Markl, D., 2021. Development of 3D Printed Rapid Tooling for Micro-Injection Moulding. *Chem. Eng. Sci.* 116498. <https://doi.org/10.1016/j.ces.2021.116498>.
- Formlabs, *Moldmaking with 3D Prints - Techniques for Prototyping and Production*, Technical Report, Formlabs, 2016.
- The International Pharmacopoeia, 5.2 Uniformity of mass for single-dose preparations, World Health Organisation (2019) 1–2. URL: <https://apps.who.int/phint/2019/index.html#p/home>.
- De Santis, F., Pantani, R., Speranza, V., Titomanlio, G., 2010. Analysis of shrinkage development of a semicrystalline polymer during injection molding. *Ind. Eng. Chem. Res.* 49, 2469–2476. <https://doi.org/10.1021/ie901316p>.
- Prasad, E., Islam, M.T., Goodwin, D.J., Megarry, A.J., Halbert, G.W., Florence, A.J., Robertson, J., 2019. Development of a hot-melt extrusion (HME) process to produce drug loaded Affinisol 15LV filaments for fused filament fabrication (FFF) 3D printing. *Addit. Manuf.* 29. <https://doi.org/10.1016/j.addma.2019.06.027>.
- Goyanes, A., Wang, J., Buanz, A., Martínez-Pacheco, R., Telford, R., Gaisford, S., Basit, A.W., 2015. 3D Printing of Medicines: Engineering Novel Oral Devices with Unique Design and Drug Release Characteristics. *Mol. Pharm.* <https://doi.org/10.1021/acs.molpharmaceut.5b00510>.
- Reynolds, T.D., Mitchell, S.A., Balwinski, K.M., 2002. Investigation of the effect of tablet surface area/volume on drug release from hydroxypropylmethylcellulose controlled-release matrix tablets. *Drug Dev. Ind. Pharm.* 28, 457–466. <https://doi.org/10.1081/DDC-120003007>.
- Zhang, J., Vo, A.Q., Feng, X., Bandari, S., Repka, M.A., 2018. Pharmaceutical Additive Manufacturing: a Novel Tool for Complex and Personalized Drug Delivery Systems. *AAPS PharmSciTech* 19, 3388–3402. <https://doi.org/10.1208/s12249-018-1097-x>.
- Zhang, J., Feng, X., Patil, H., Tiwari, R.V., Repka, M.A., 2017. Coupling 3D printing with hot-melt extrusion to produce controlled-release tablets. *Int. J. Pharm.* 519, 186–197. <https://doi.org/10.1016/j.ijpharm.2016.12.049>.
- Korte, C., Quodbach, J., 2018. Formulation development and process analysis of drug-loaded filaments manufactured via hot-melt extrusion for 3D-printing of medicines. *Pharm. Dev. Technol.* 23, 1117–1127. <https://doi.org/10.1080/10837450.2018.1433208>.
- Aho, J., Bötter, J.P., Genina, N., Edinger, M., Arnfast, L., Rantanen, J., 2019. Roadmap to 3D-Printed Oral Pharmaceutical Dosage Forms: Feedstock Filament Properties and Characterization for Fused Deposition Modeling. *J. Pharm. Sci.* 108, 26–35. <https://doi.org/10.1016/j.xphs.2018.11.012>.
- Gioumouxouzis, C.I., Karavasili, C., Fatouros, D.G., 2019. Recent advances in pharmaceutical dosage forms and devices using additive manufacturing technologies. *Drug Discovery Today* 24, 636–643. <https://doi.org/10.1016/j.drudis.2018.11.019>.
- Zheng, Y., Deng, F., Wang, B., Wu, Y., Luo, Q., Zuo, X., Liu, X., Cao, L., Li, M., Lu, H., Cheng, S., Li, X., 2021. Melt extrusion deposition (med) 3d printing technology – a paradigm shift in design and development of modified release drug products. *Int. J. Pharm.* 602, 120639. <https://doi.org/10.1016/j.ijpharm.2021.120639>.
- Pires, F.Q., Alves-Silva, I., Pinho, L.A., Chaker, J.A., Sa-Barreto, L.L., Gelfuso, G.M., Gratieri, T., Cunha-Filho, M., 2020. Predictive models of FDM 3D printing using experimental design based on pharmaceutical requirements for tablet production. *Int. J. Pharm.* 588, 119728. <https://doi.org/10.1016/j.ijpharm.2020.119728>.
- Rahmati, S., Dickens, P., 2007. Rapid tooling analysis of Stereolithography injection mould tooling. *Int. J. Mach. Tools Manuf* 47, 740–747. <https://doi.org/10.1016/j.ijmachtools.2006.09.022>.